Particularities of Black Hole shadows when spinning is taken into account

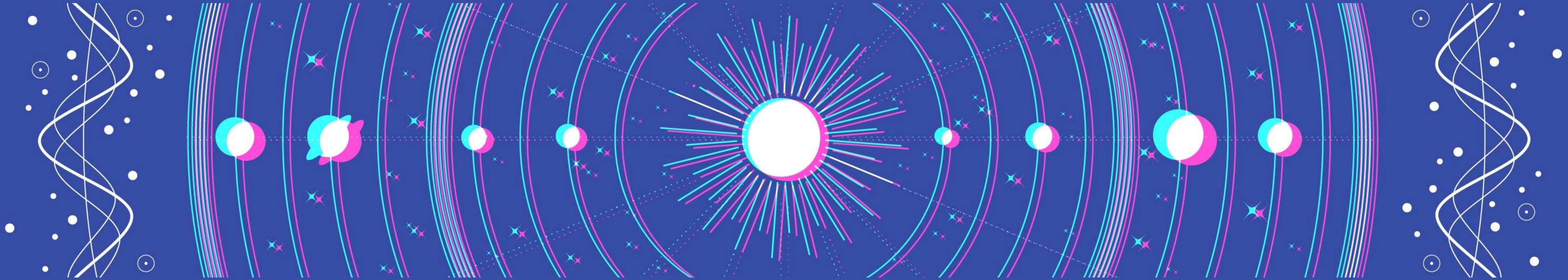

Oleg Zenin (Faculty of Physics MSU)
Stanislav Alexeyev (SAI MSU)
Artem Baiderin (Faculty of Physics MSU)

Introduction

The existence of black holes was proven by:

- results on binary systems dynamics
- gravitational wave astronomy
- direct imaging of black hole

The first recorded gravitational waves from the BH merger*

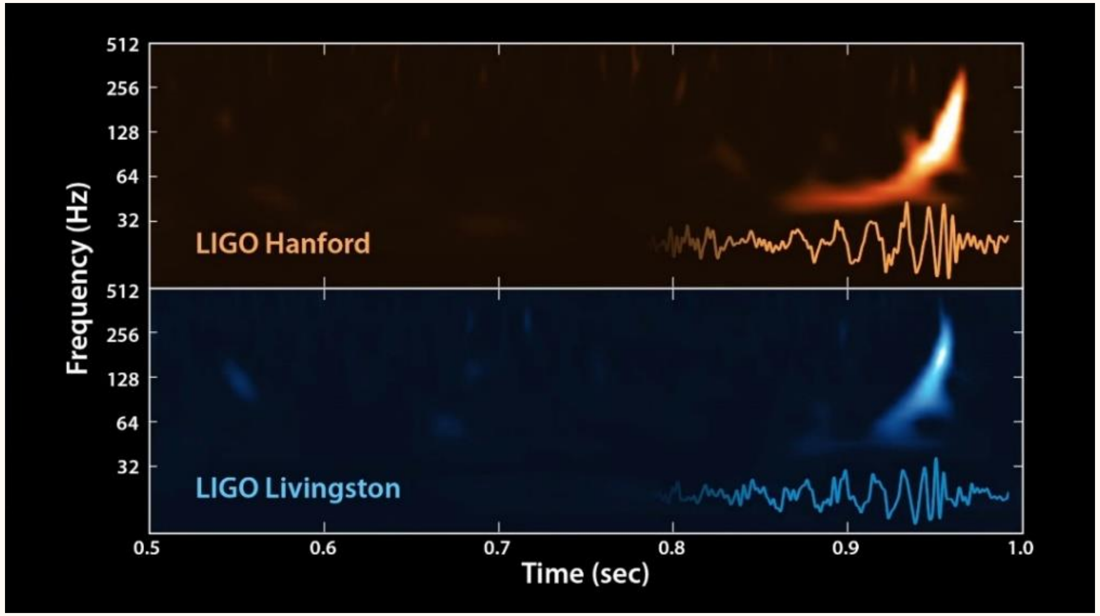

** B.P. Abbott et al. Phys. Rev. D, 93(12):122003, 2016.*

Introduction

M 87*

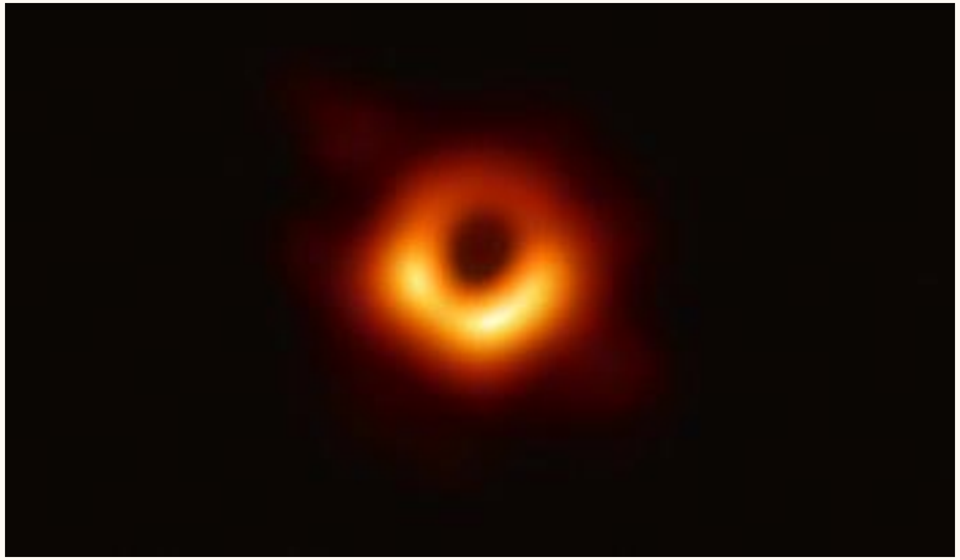

BH shadow size from 4.3M to 6.1M

K. Akiyama, et al., Astrophys. J. 875 (1) L5 (2019).

Sgr A*

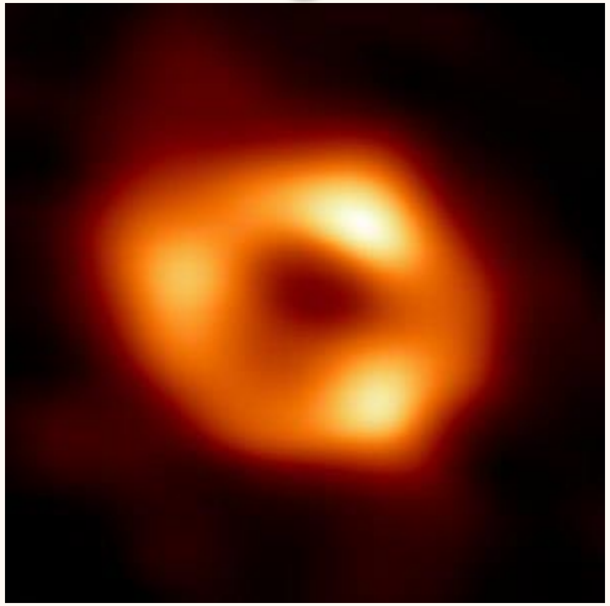

BH shadow size from 4.3M to 5.3M

The Event Horizon Telescope Collaboration, The Astrophysical Journal Letters 930 L17 (2022).

Newman–Janis algorithm

Metric function:

$$ds^2 = -G(r)dt^2 + \frac{1}{F(r)}dr^2 + H(r)d\Omega^2. \qquad (1)$$

New metric:

$$g_{tt} = -\frac{FH + a^2\cos^2\theta}{(K + a^2\cos^2\theta)^2}\Psi,$$

$$g_{t\phi} = -a\sin^2\theta\frac{K - FH}{(K + a^2\cos^2\theta)^2}\Psi,$$

$$g_{\theta\theta} = \Psi,$$

$$g_{rr} = \frac{\Psi}{FH + a^2}, \qquad (2)$$

$$g_{\phi\phi} = \Psi\sin^2\theta(1 + a^2\sin^2\theta\frac{2K - FH + a^2\cos^2\theta}{(K + a^2\cos^2\theta)^2}).$$

$$K = H(r)\sqrt{F(r)/G(r)}.$$

$$y \equiv \cos\theta.$$

$\Psi(r, y^2, a)$ Conditions:

$$\lim_{a\to 0}\Psi(r, y^2, a) = H(r),$$
$$(K + a^2y^2)^2(3\Psi_r\Psi_{y^2} - 2\Psi\Psi_{r,y^2}) = 3a^2K_r\Psi^2,$$
$$\Psi\left[K_r^2 + K(2 - K_{rr}) - a^2y^2(2 + K_{rr})\right] +$$
$$+ (K + a^2y^2)[(4y^2\Psi_{y^2} - K_r\Psi_r] = 0. \qquad (3)$$

$$ds_c^2 = \Psi_c/\Psi_n ds_n^2. \qquad (4)$$

Solution of equation (3):

$$\Psi_c = H(r)\exp\left[a^2 f(r, a^2y^2, a)\right] \approx$$
$$\approx H(r) + a^2X(y^2, r) + o(a^2), \qquad (5)$$

$$A_r = \partial A/\partial r$$

$$KH_rK_r + HK_r^2 + HK(K_{rr} - 2) = 0,$$
$$X(y^2, r) = \frac{H^2(8K - K_r^2)y^2}{K^2(8H - H_rK_r)},$$
$$K_r(8K - K_r^2)K_{rrr} + K_r^2(K_{rr} - 2)^2 -$$
$$- 4KK_{rr}(K_{rr} + 4) + 48K = 0. \qquad (6)$$

3 The modelling of BH shadow: how to include the rotation

Coordinates of the BH shadow on a plane perpendicular to the observer's line of sight

Shadow of rotation black hole image and photon geodesics

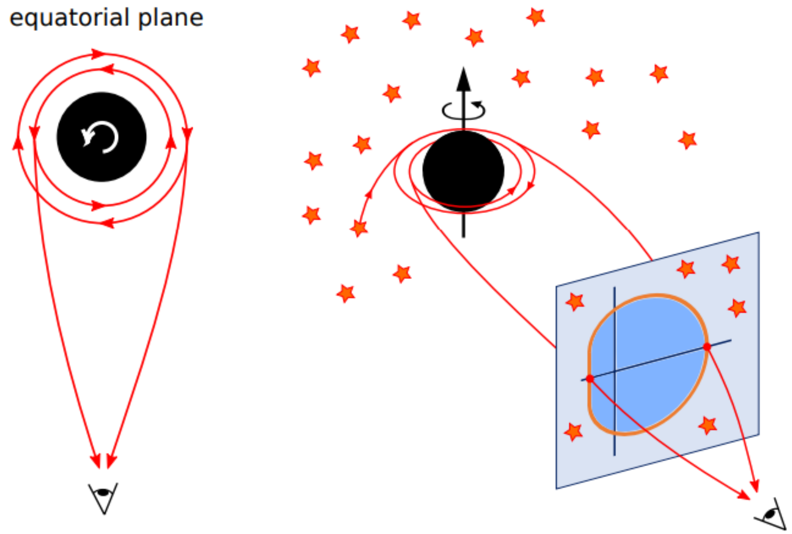

$$x' = -\frac{\lambda}{\sin\theta_0},$$

$$y' = \pm\sqrt{\eta + a^2\cos^2\theta_0 - \frac{\lambda^2}{\tan^2\theta_0}},$$

$$\lambda = \frac{\omega + a^2}{a} - \frac{2\omega'}{a}\frac{(f_r^{-1}r^2 + a^2)}{(f_r^{-1}r^2)'},$$

$$\eta = \frac{4(f_r^{-1}r^2 + a^2)}{(f_r^{-1}r^2)'^2}\omega'^2 - \frac{1}{a^2}\left[\omega - \frac{2(f_r^{-1}r^2 + a^2)}{(f_r^{-1}r^2)'}\omega'\right]^2,$$

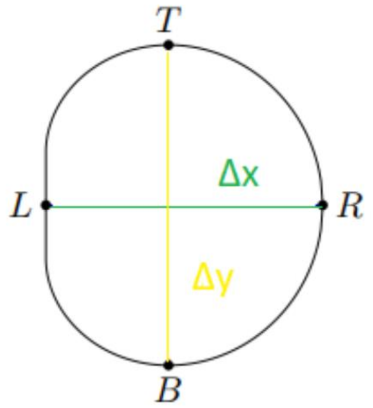

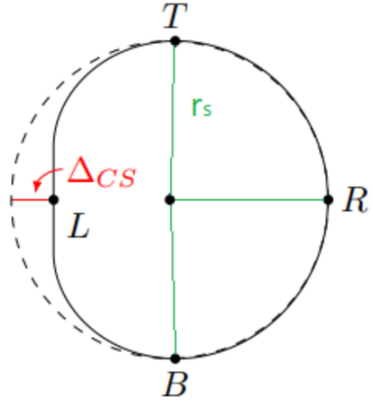

$$D = \frac{x_{min} + x_{max}}{2},$$

D – shift parameter

$$\delta_{cs} = \Delta_{cs}/r_s,$$

δ_{cs} – distortion parametr

Volker Perlick, Oleg Yu. Tsupko, Physics Reports, Volume 947, 2022, Pages 1-39

K. Hioki and Kei-ichi Maeda, Phys. Rev. D **80**, 024042 (2009).

4

Black hole shadows

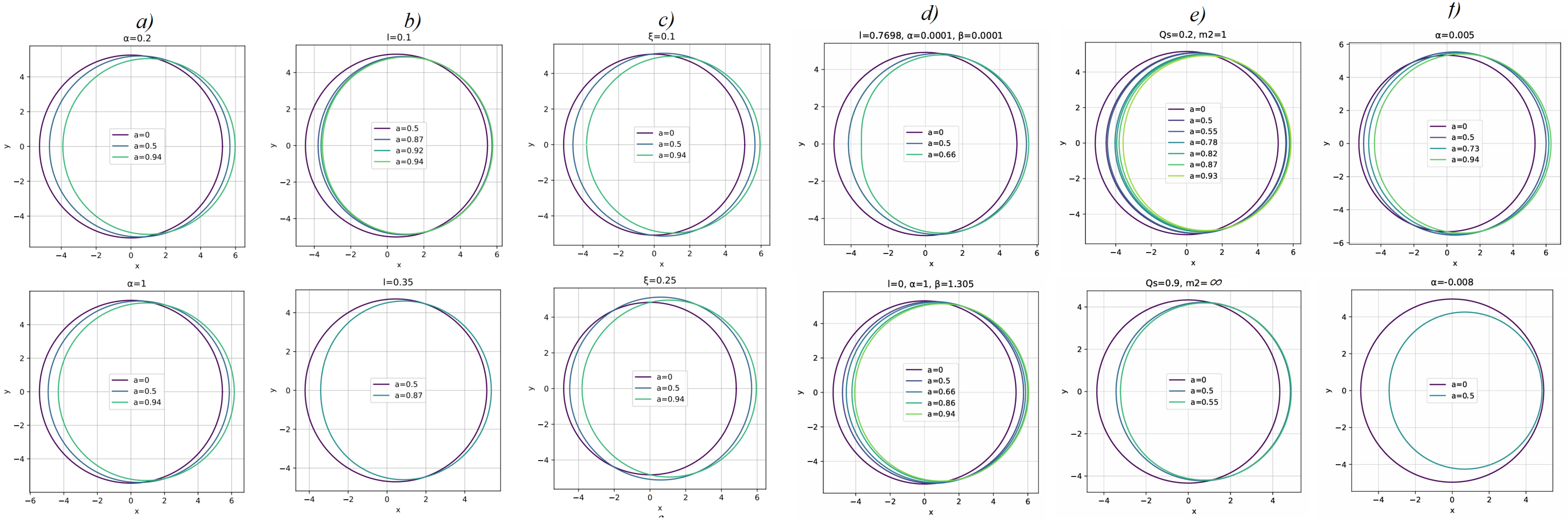

a

Horndeski Theory

$$S = \int \sqrt{-g} d^4x (\mathcal{L}_2 + \mathcal{L}_3 + \mathcal{L}_4 + \mathcal{L}_5 + \mathcal{L}_4^{bH} + \mathcal{L}_5^{bH}),$$

$$\mathcal{L}_2 = G_2(X),$$
$$\mathcal{L}_3 = -G_3(X)\Box\phi,$$
$$\mathcal{L}_4 = G_4(X)R + G_{4X}[(\Box\phi)^2 - (\nabla_\mu\nabla_\nu\phi)^2],$$
$$\mathcal{L}_5 = G_5(X)G_{\mu\nu}\nabla^\mu\nabla^\nu - \frac{1}{6}G_{5X}[(\Box\phi)^3 - 3\Box\phi(\nabla_\mu\nabla_\nu\phi)^2 + 2(\nabla_\mu\nabla_\nu\phi)^3],$$
$$\mathcal{L}_4^{bH} = F_4(X)\epsilon^{\mu\nu\rho\sigma}\epsilon_\sigma^{\alpha\beta\gamma}\nabla_{\mu\phi}\nabla_{\alpha\phi}\nabla_\nu\nabla_{\beta\phi}\nabla_\rho\nabla_{\gamma\phi}\nabla_\sigma\nabla_{\delta\phi},$$
$$\mathcal{L}_5^{bH} = F_5(X)\epsilon^{\mu\nu\rho\sigma}\epsilon^{\alpha\beta\gamma\delta}\nabla_{\mu\phi}\nabla_{\alpha\phi}\nabla_\nu\nabla_{\beta\phi}\nabla_\rho\nabla_{\gamma\phi}\nabla_\sigma\nabla_{\delta\phi}\nabla_\sigma\nabla_{\delta\phi}.$$

$$A(r) = 1 - \frac{2M}{r} - \frac{2C_7}{7r^7},$$
$$B(r)^{-1} = 1 - \frac{2M}{r} - \frac{C_7}{r^7},$$

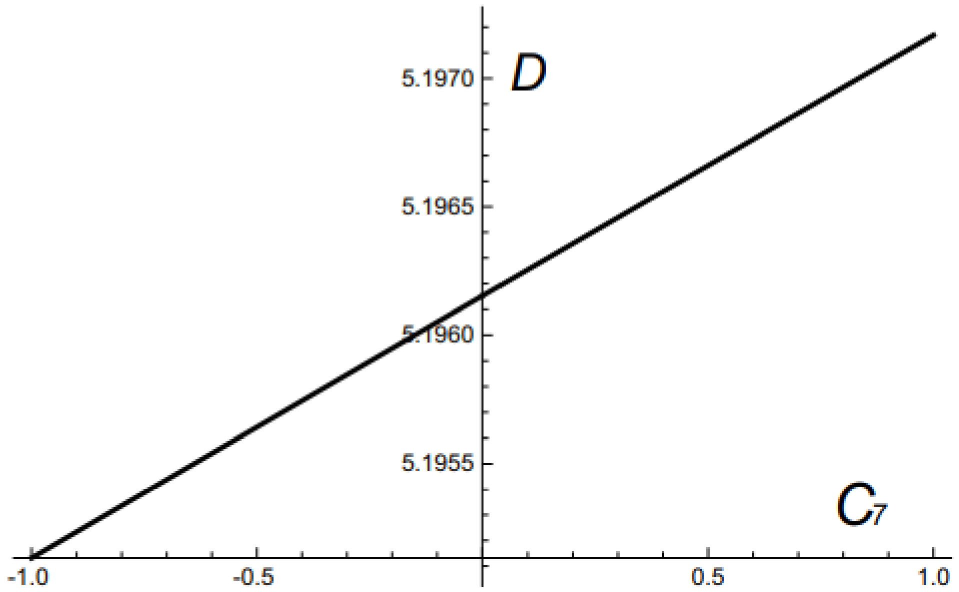

Fig. 3. The dependence of shadow size (D) versus the combination of model constants C_7 for Horndesky theory coupled with Gauss-Bonnet invariant (in the units of M, $M = 1$).

[12] Eugeny Babichev, Christos Charmousis, and Antoine Lehébel. Asymptotically flat black holes in Horndeski theory and beyond. JCAP, 04:027, 2017.

Prokopov V. A., Alexeyev S. O ., O. Z., JETP. — 2022. — Vol. 135, no. 1. — P. 91–99.

a

Horndeski Theory (rotation)

$$g_{tt} = -\left(1 - \frac{2Mr}{\rho^2} - \frac{8\alpha_5\eta}{5r}\right),$$

$$g_{t\phi} = -\frac{2a\sin^2\theta}{5r\rho^2}\left(4\alpha_5\eta + 9Mr^2\right),$$

$$g_{rr} = \rho^2\left(-\frac{8\alpha_5\eta}{5r} + a^2 - 2Mr + r^2\right)^{-1},$$

$$g_{\theta\theta} = \rho^2,$$

$$g_{\phi\phi} = \frac{\sin^2\theta}{\rho^2}\Big(r^4 + 2ar^2\cos^2\theta + a^4\cos^4\theta + + \frac{8a^2\alpha_5\eta\sin^2\theta}{5r} + 2aMr\sin^2\theta + + a^2r^2\sin^2\theta + a^4\cos^2\theta\sin^2\theta\Big),$$

$$\alpha = 8\alpha_5\eta/5$$

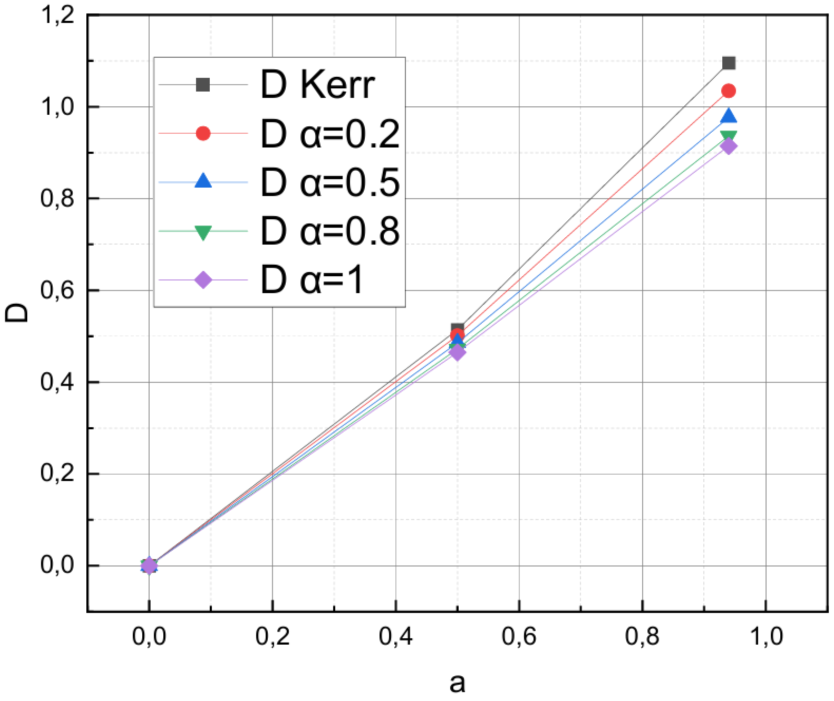

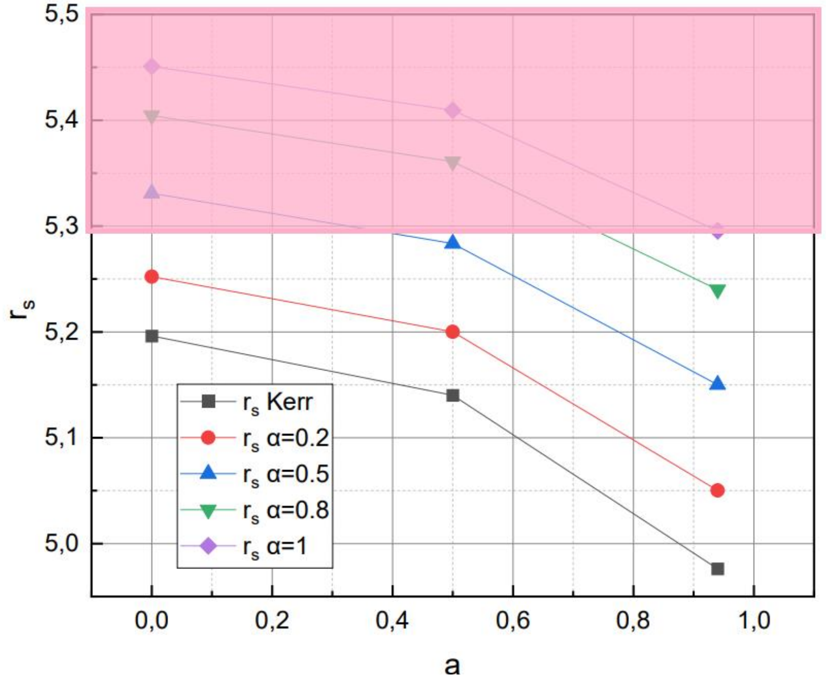

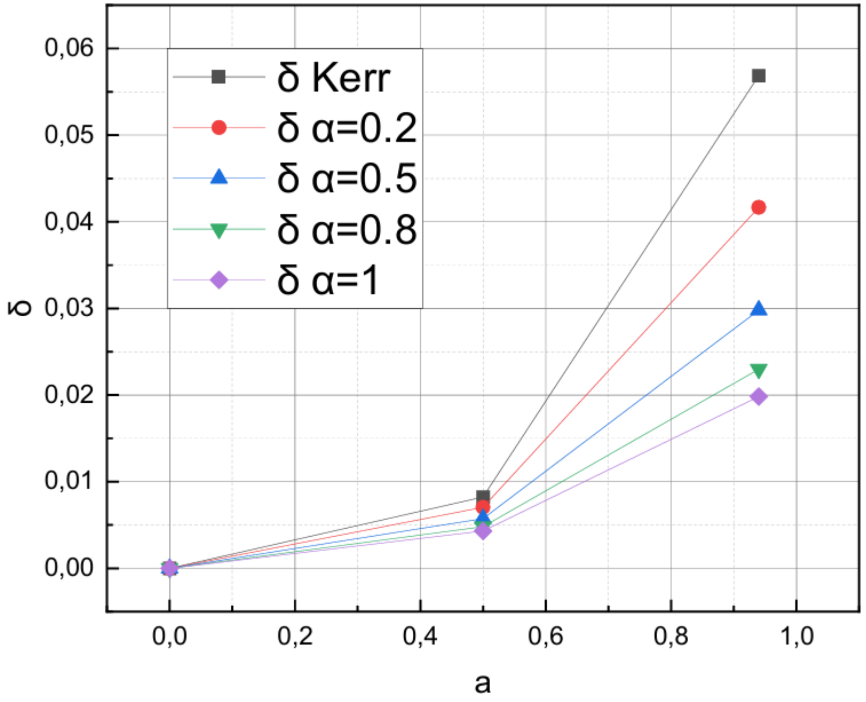

b

Bumblebee mode

$$S_B = \int d^4x \mathcal{L}_B = \int d^4x (\mathcal{L}_g + \mathcal{L}_{gB} + \mathcal{L}_K + \mathcal{L}_V + \mathcal{L}_M),$$

$$A(r) = (1+l)(1-\frac{2M}{r}),$$
$$B(r)^{-1} = 1-\frac{2M}{r}.$$

$-0,05 < l < 0,45$

[26] R. Casana, A. Cavalcante, F. P. Poulis, and E. B. Santos. Exact schwarzschild-like solution in a bumblebee gravity model. Physical Review D, 97(10), 2018.

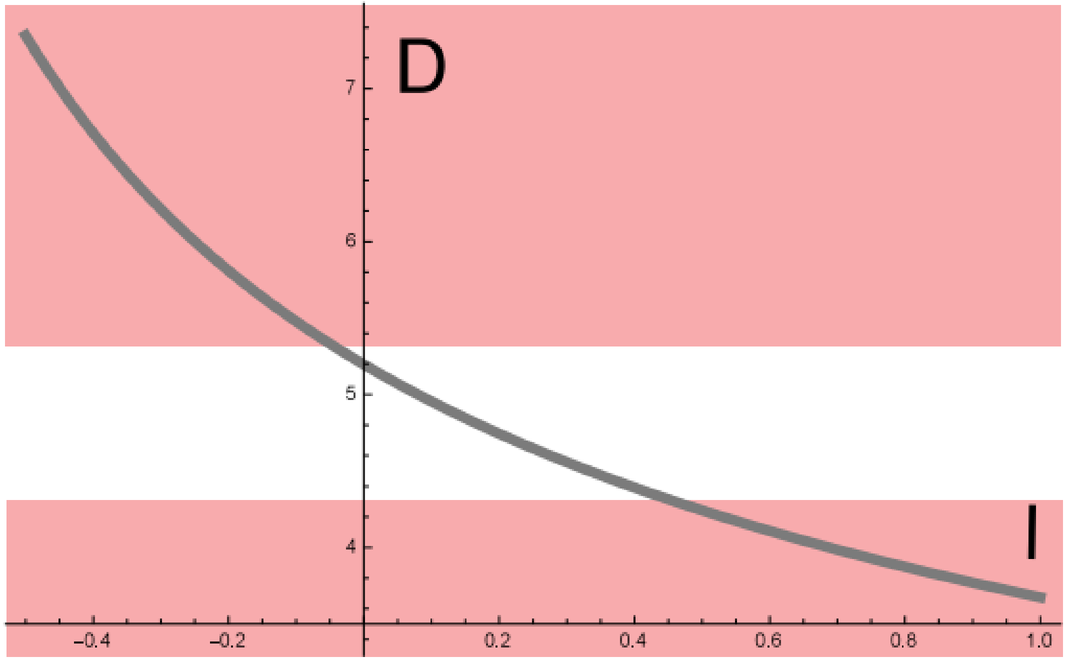

Рис. 1. The dependence of the shadow size D upon parameter l in alternative bumblebee generalization with Schwarzschild approximation (in the units of M, $M = 1$).

Prokopov V. A., Alexeyev S. O., Zenin O. I. Black hole shadows constrain extended gravity 2: Sgr a* // *JETP*. — 2022.

b

Bumblebee mode (rotation)

$$
\begin{aligned}
g_{tt} &= \frac{r^{-1+\sqrt{1+l}}AB}{\sqrt{1+l}CD},\\
g_{t\phi} &= -\frac{ar^{-l+\sqrt{1+l}}EB\sin^2\theta}{(1+l)CD},\\
g_{rr} &= \frac{(1+l)r^{-l+\sqrt{1+l}}B}{CG},\\
g_{\theta\theta} &= r^{1+\sqrt{1+l}} + \frac{a^2(-4+8\sqrt{1+l})r^{-l+\sqrt{1+l}}\cos^2\theta}{8-2(1+\sqrt{1+l})},\\
g_{\phi\phi} &= \frac{r^{-l+\sqrt{1+l}}\sin^2\theta(B+5a^2\cos^2\theta)}{(1+l)CD}\times\\
&\times\Big(D(1+l)-Ka^2\cos^2\theta\Big),
\end{aligned}
$$

$$
\begin{aligned}
&A = (2Mr^{1+l} - r^{1+\sqrt{1+l}} - a^2\cos^2\theta - a^2 l\cos^2\theta),\\
&B = -3r^2 + \sqrt{1+l}r^2 - 3a^2\cos^2\theta - 4a^2\sqrt{1+l}\cos^2\theta,\\
&C = -3+\sqrt{1+l}, \qquad D = r^2 + a^2\sqrt{1+l}\cos^2\theta,\\
&E = -r^2 - lr^2 - 2\sqrt{1+l}Mr^{\sqrt{1+l}} + \sqrt{1+l}r^{1+\sqrt{1+l}},\\
&G = a^2 + a^2 l - 2Mr^{1+l} + r^{1-\sqrt{1+l}},\\
&F = -2Mr^{\sqrt{1+l}} + r^{1+\sqrt{1+l}} - a^2 l\cos^2\theta,\\
&K = \sqrt{1+l}F - r - 2lr^2 - D.
\end{aligned}
$$

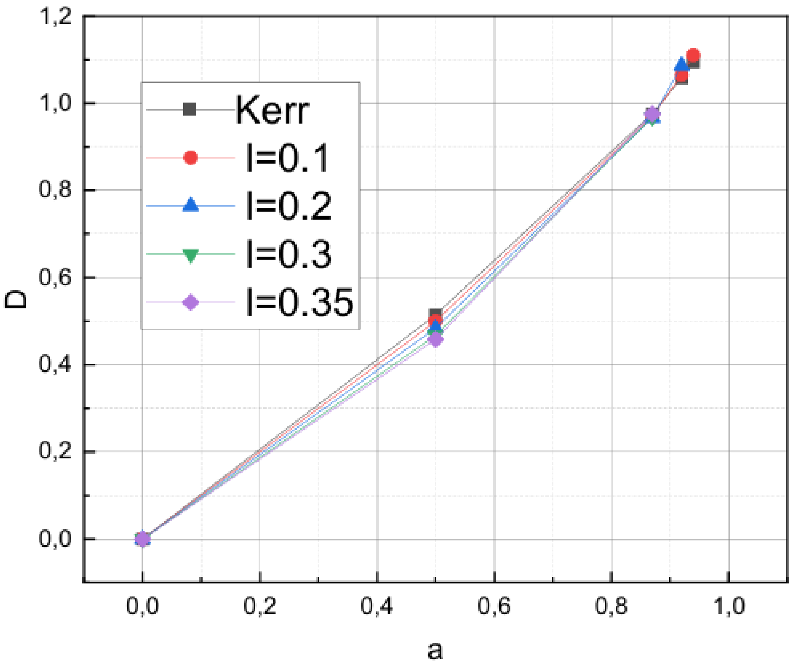

$l=0.35 \quad a_{crit}=0.87$

$l=0.2 \quad a_{crit}=0.92$

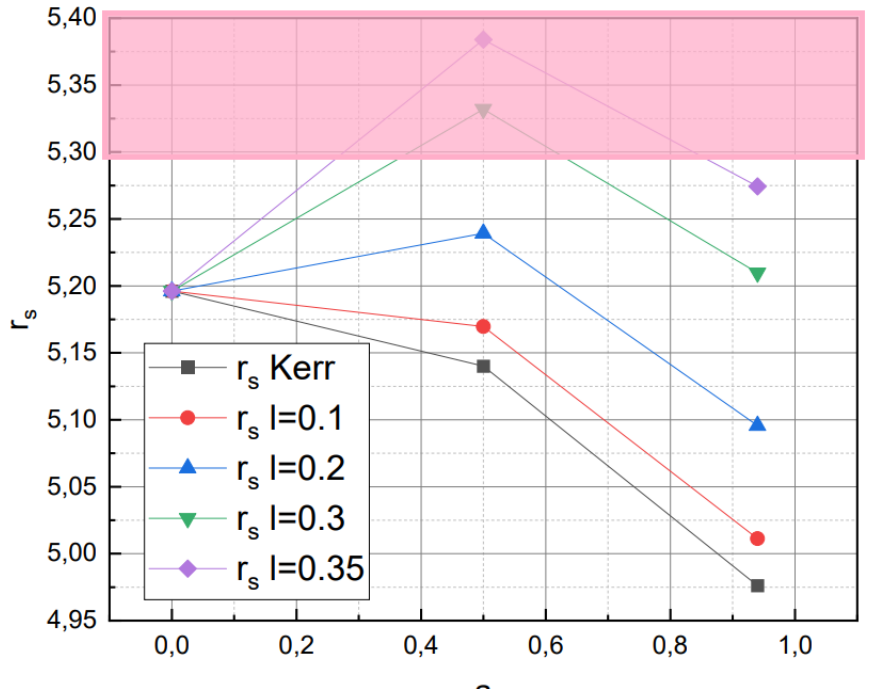

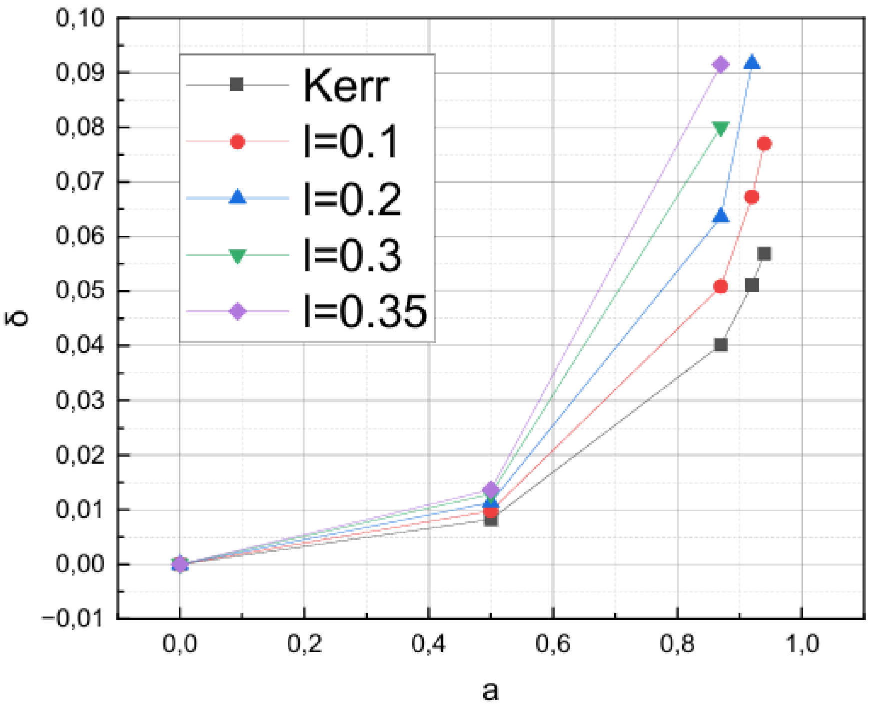

C

Scalar Gauss-Bonnet gravity

$$A = -f(r)[1 + \frac{\zeta}{3r^3 f(r)} h(r)], \qquad (34)$$

$$B = \frac{1}{f(r)}[1 - \frac{\zeta}{r^3 f(r)} k(r)], \qquad (35)$$

where

$$h(r) := 1 + \frac{26}{r} + \frac{66}{5r^2} + \frac{96}{5r^3} - \frac{80}{r^4}, \qquad (36)$$

$$k(r) := 1 + \frac{1}{r} + \frac{52}{3r^2} + \frac{2}{r^3} + \frac{16}{5r^4} - \frac{368}{3r^5}, \qquad (37)$$

$$f(r) := 1 - \frac{2}{r}, \qquad (38)$$

where ζ is the coupling parameter.

[18] Nicolás Yunes and Leo C. Stein. Nonspinning black holes in alternative theories of gravity. Phys. Rev. D, 83:104002, 2011.

Dependences of the radius of the photonic sphere and the radius of BH shadowon the coupling parameter in the first order:

$$r_{ph}^{sGB} = 3[1 - \frac{961}{2430}\zeta],$$

$$b_c^{sGB} = \sqrt{27}[1 - \frac{4397\zeta}{21870}].$$

[50] Adam Bauer, Alejandro Cárdenas-Avendaño, Charles F. Gammie, and Nicolás Yunes. Spherical accretion in alternative theories of gravity, 2021.

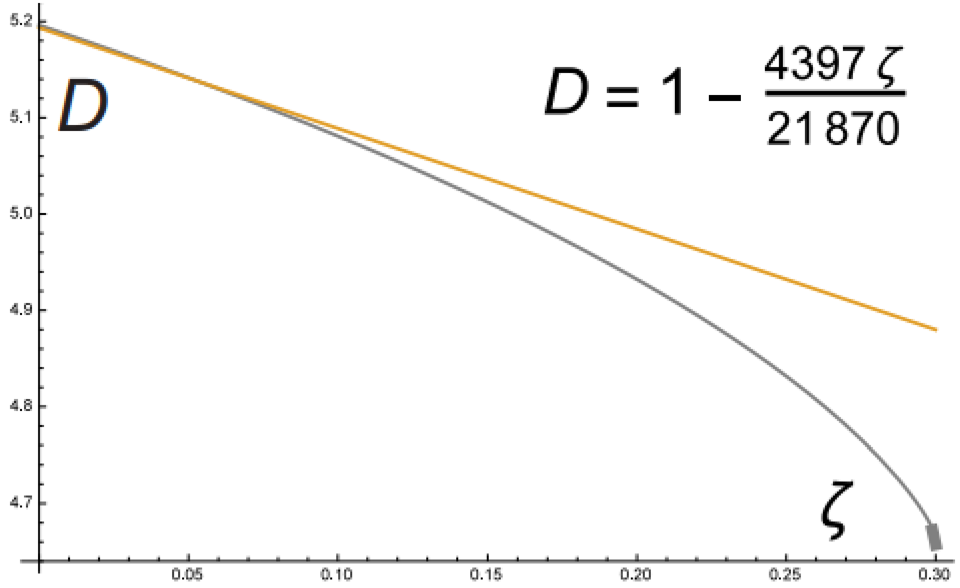

Fig. 8. The lower curve is the dependence of the shadow size D upon parameter ζ in scalar Gauss-Bonnet gravity (in the units of M, $M = 1$). The top line is the first order approximation.

Prokopov V. A., Alexeyev S. O ., O. Z., JETP. — 2022. — Vol. 135, no. 1. — P. 91–99.

c

Scalar Gauss-Bonnet gravity (rotation)

$$g_{tt} = \frac{r^2(E + F\cos^2\theta)}{AB},$$
$$g_{t\phi} = -\frac{aCD\sin^2\theta}{AB},$$
$$g_{rr} = -\frac{AB}{r^2(E+F)},$$
$$g_{\theta\theta} = \frac{B}{3r^2},$$
$$g_{\phi\phi} = \frac{T}{3r^2 AB},$$

$$A = \xi + 2Mr^2 - r^3,$$
$$B = 2\xi M + \xi r + 3r^4 + 3a^2r^2\cos^2\theta,$$
$$C = 2\xi M + \xi r + 3r^4,$$
$$D = A + 16M^2r^2 - 16Mr^4 + 4r^5,$$
$$E = 32\xi M^3 r - 16\xi M^2 r^2 - 8\xi M r^3 + 4\xi r^4 + + 48M^2r^5 - 48Mr^6 + 12r^7,$$
$$F = -3a^2\xi - 6a^2Mr^2 + 3a^2r^3,$$
$$G = 16\xi M^3 r^5 + 2\xi r^6 + 24M^2r^7 - 24Mr^8 + 6r^9,$$
$$K = 2\xi^2 M + \xi^2 r + 4\xi M^2 r^2 + 2\xi r^4 + 6Mr^6 - 3r^7,$$
$$Q = 4\xi^3 M(M+r) + \xi^2 r^2(\xi + 2M^3 + 4M^2 r + + 10Mr^2 + 5r^3) + 3\xi r^6(8M^2 + r^2) + 9r^{10}(2M - r),$$
$$T = 1 + Q + 9a^4r^4 A\cos^4\theta + 6a^2r^2 G\sin^2\theta + + 9a^4r^4 A\cos^2\theta\sin^2\theta.$$

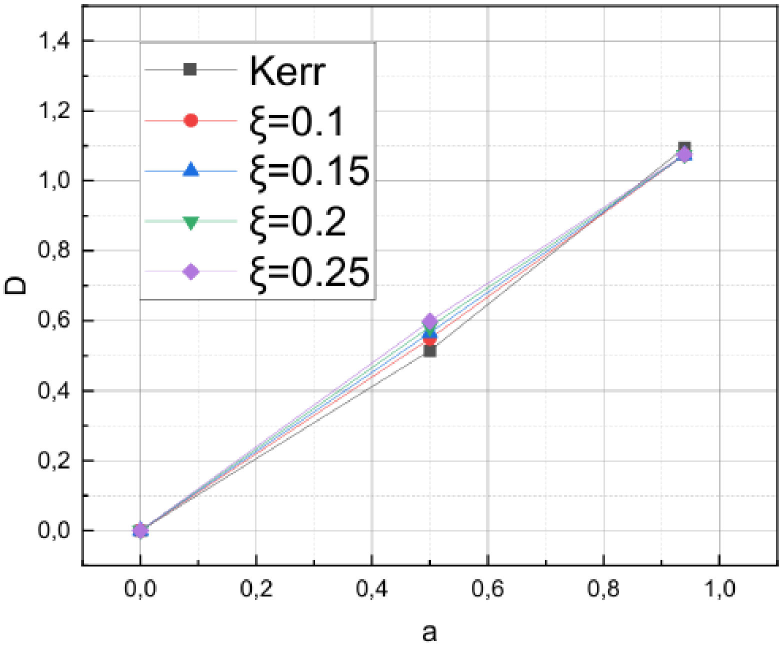

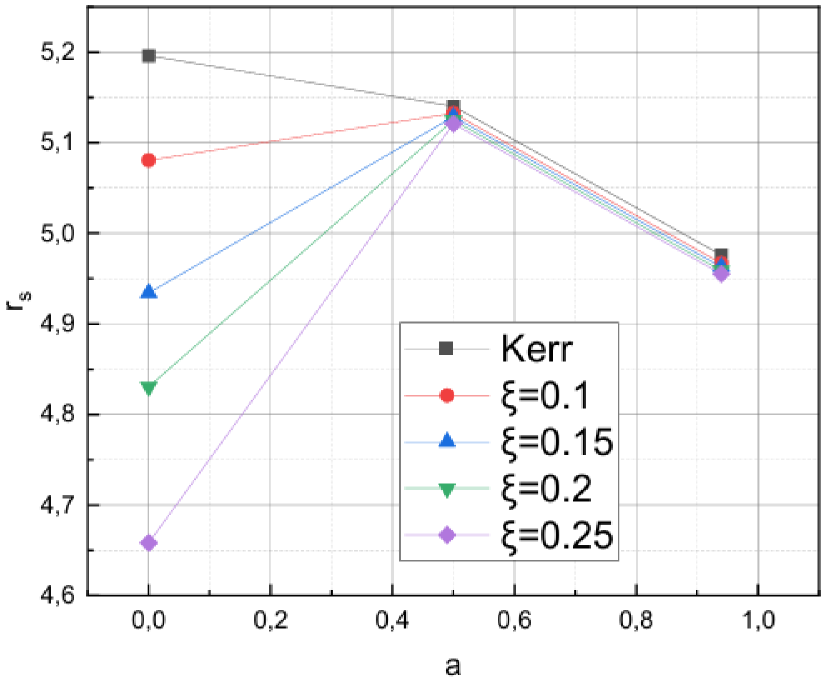

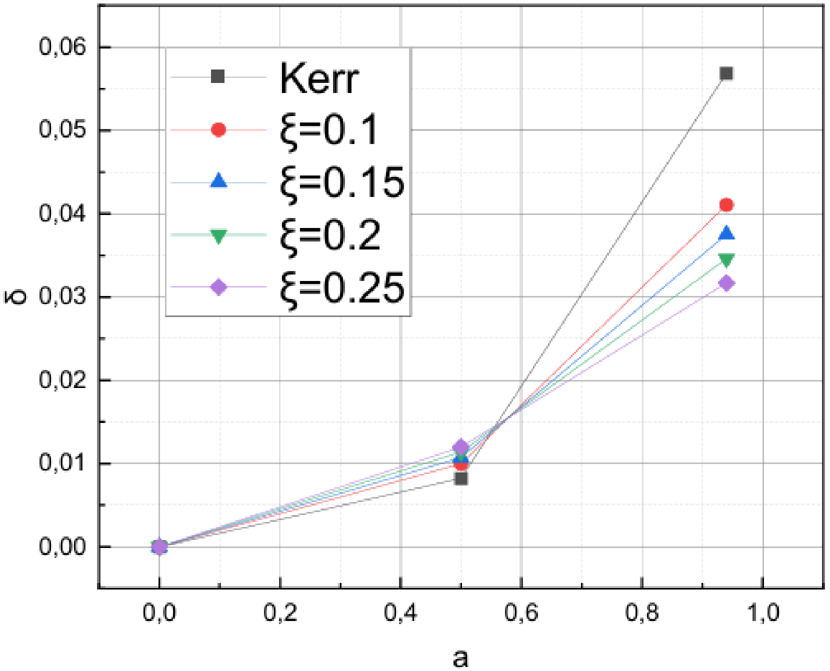

d

Loop Quantum Gravity

$$A(r) = (1 - \frac{2Mr^2}{r^3 + 2Ml^2})(1 - \frac{\alpha\beta M}{\alpha r^3 + \beta M})$$

$$B(r)^{-1} = 1 - \frac{2Mr^2}{r^3 + 2Ml^2}$$

where l encodes the central energy density $3/8\pi l^2$,

$0 \leq \alpha < 1, \ \beta_{max} = 41/(10\pi) \approx 1.305$

$l > \sqrt{16/27}M \approx 0.7698$

[17] Jian-Ping Hu, Li-Li Shi, Yu Zhang, and Peng-Fei Duan. Analytical time-like geodesics in modified hayward black hole space-time. Astrophysics and Space Science, 363(10), 2018.

Prokopov V. A., Alexeyev S. O ., O. Z., JETP. — 2022. — Vol. 135, no. 1. — P. 91–99.

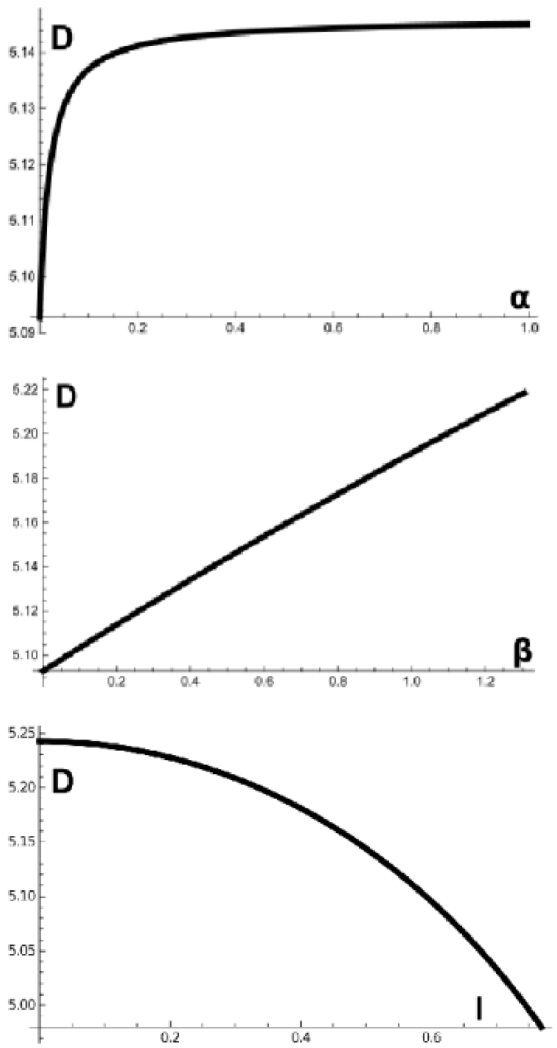

Fig. 4. The dependence of shadow size D upon the time delay α when $l = 0.5M$ and $\beta = 0.5$ (top image), upon the 1-loop quantum corrections β when $l = 0.5M$, $\alpha = 0.5$ (central image), upon the central energy density l when $\alpha = 0.5$, $\beta = 0.5$ (bottom image) for BH in modified Hayward metric in the units of M, $M = 1$.

d

Loop Quantum Gravity (rotation)

$$g_{tt} = -\frac{\rho^2 - A}{B},$$

$$g_{t\phi} = -a \sin^2\theta \frac{\tilde{H} - r^2(1-A)}{B},$$

$$g_{\theta\theta} = B,$$

$$g_{rr} = \frac{B}{r^2 + a^2 - A},$$

$$g_{\phi\phi} = \sin^2\theta \left(B + a^2 \sin^2\theta \frac{2\tilde{H} - 2r^2 + \rho^2 + r^2 A}{B} \right)$$

$$\tilde{H}(r) = r^2 \left(1 - \frac{M\alpha\beta}{\alpha r^3 + \beta M}\right)^{-1/2},$$

$$A = 2Mr^2 \left(r^3 + 2Ml^2\right)^{-1},$$

$$B = \tilde{H} + a^2 \cos^2\theta.$$

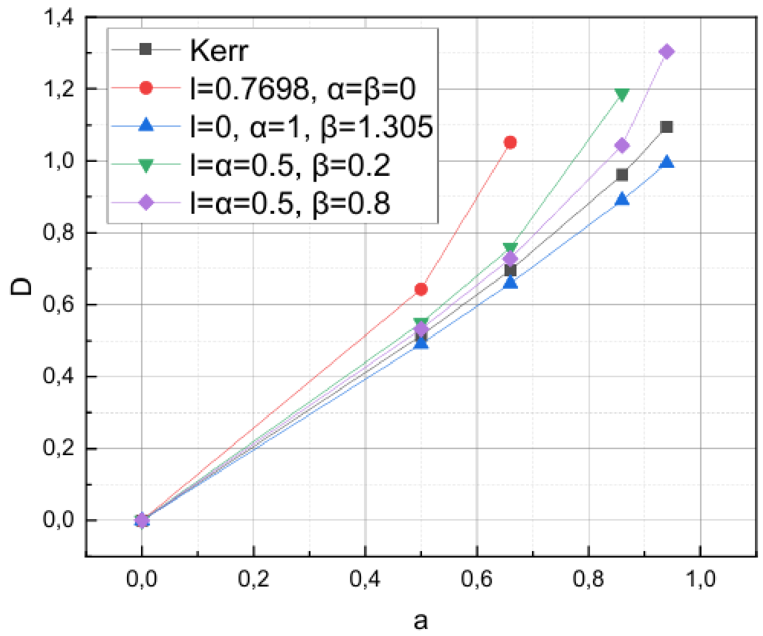

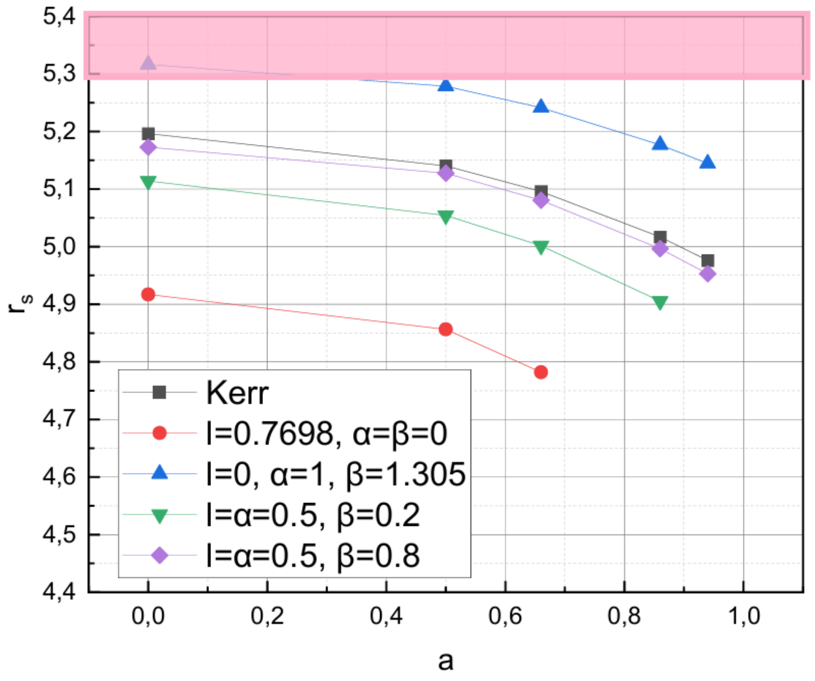

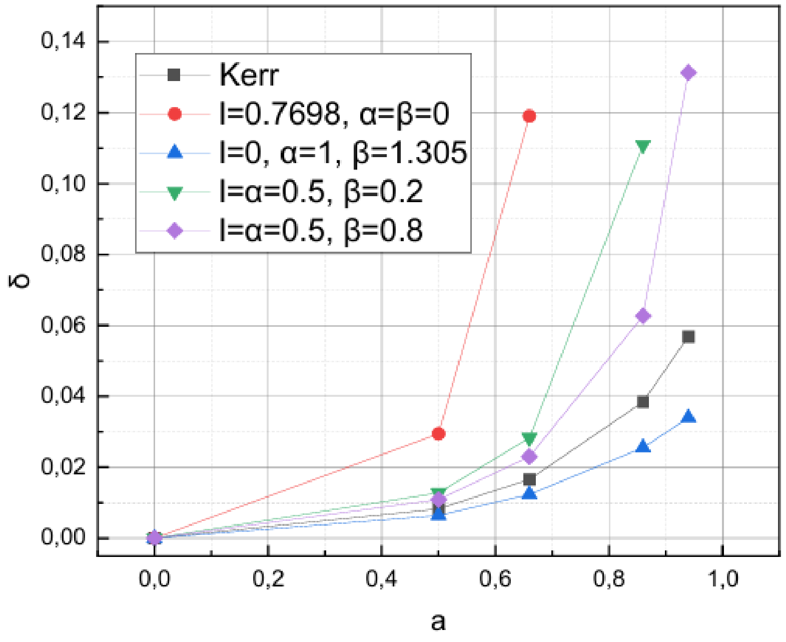

$l=0.7698,\ \alpha=\beta=0 \quad a_{crit}=0.66$

$l=\alpha=0.5,\ \beta=0.2 \quad a_{crit}=0.86$

e

Conformal Gravity

$$S = \frac{1}{16\pi G}\int d^4x\sqrt{-g}[R - \alpha(\phi^2 R + 6\partial_\mu\phi\partial^\mu\phi] - \frac{1}{2m_2^2}C^{\mu\nu\rho\sigma}C_{\mu\nu\rho\sigma}],$$

$$A(r) = 1 - \frac{2M}{r} + \frac{Q_s^2}{r^2} + \frac{Q_s^2(-M^2 + Q_s^2 + \frac{6}{m_2^2})}{3r^4} + \dots$$

$$B(r)^{-1} = 1 - \frac{2M}{r} + \frac{Q_s^2}{r^2} + \frac{2Q_s^2(-M^2 + Q_s^2 + \frac{6}{m_2^2})}{3r^4} + \dots,$$

if m_2=2, Q_s<0,9

[14] Yun Soo Myung and De-Cheng Zou. Black holes in new massive conformal gravity. Physical Review D, 100(6), 2019.

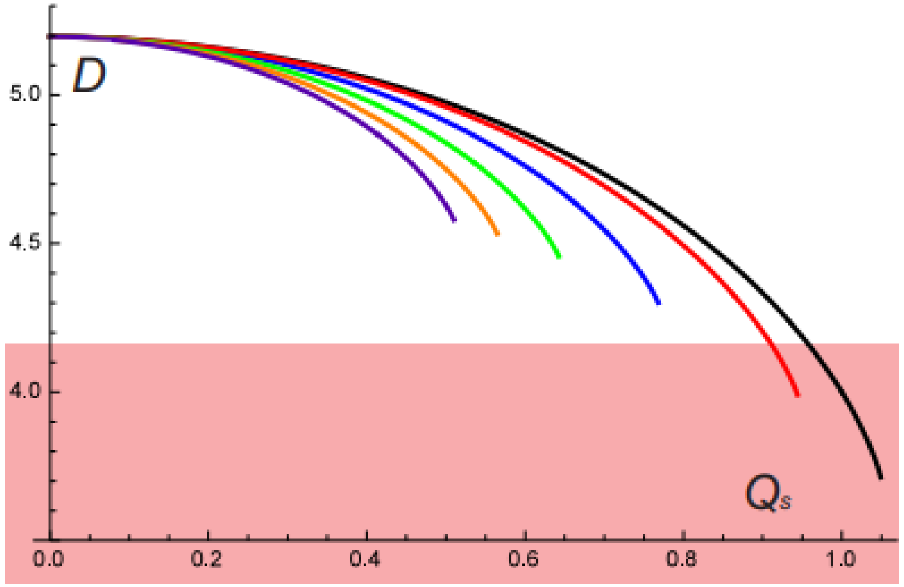

Fig. 5. The dependence of the shadow size D against the scalar charge Q_s for in new massive conformal gravity with different values of massive spin-2 mode m_2 (in the units of M, $M = 1$). Black line corresponds to $m_2 \to \infty$, red one corresponds to $m_2 = 2$, blue one corresponds to $m_2 = 1$, green one corresponds to $m_2 = 0.707$, orange one corresponds to $m_2 = 0.577$, purple one corresponds to $m_2 = 0.5$.

Prokopov V. A., Alexeyev S. O ., O. Z., JETP. — 2022. — Vol. 135, no. 1. — P. 91–99.

e

Conformal Gravity (rotation)

$$g_{tt} = -\frac{\rho^2 + A^2}{\rho^2},$$

$$g_{t\phi} = a \sin^2\theta \frac{A^2}{\rho^2},$$

$$g_{\theta\theta} = \rho^2,$$

$$g_{rr} = \frac{\rho^2}{r^2 + a^2 + A^2},$$

$$g_{\phi\phi} = \sin^2\theta \left(\rho^2 + a^2 \sin^2\theta \frac{\rho^2 - A^2}{\rho^2}\right),$$

$$A^2 = -2Mr + Q_s^2 + \frac{2}{3}\frac{Q_s^2}{r^2}\left(Q_s^2 - M^2 + 6m_2^{-2}\right)$$

$m_2=2$, $Q_s=0.73$ $a_{crit}=0.5$

$m_2=2$, $Q_s=0.5$ $a_{crit}=0.82$

$m_2=\infty$, $Q_s=0.9$ $a_{crit}=0.55$

$m_2=\infty$, $Q_s=0.5$ $a_{crit}=0.93$

$m_2=1$, $Q_s=0.51$ $a_{crit}=0.5$

$m_2=1$, $Q_s=0.35$ $a_{crit}=0.78$

$m_2=1$, $Q_s=0.2$ $a_{crit}=0.93$

$m_2=0.707$, $Q_s=0.39$ $a_{crit}=0.5$

$m_2=0.707$, $Q_s=0.2$ $a_{crit}=0.87$

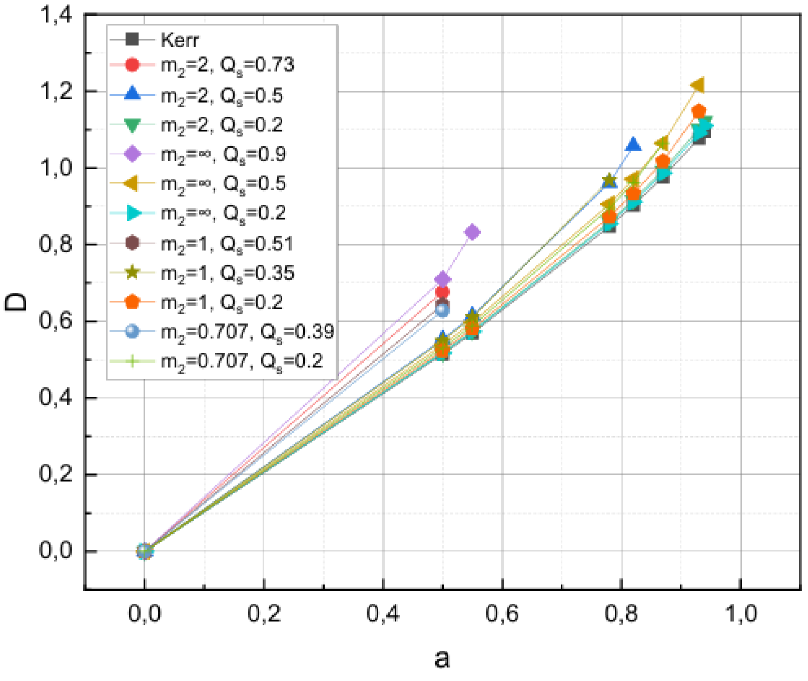

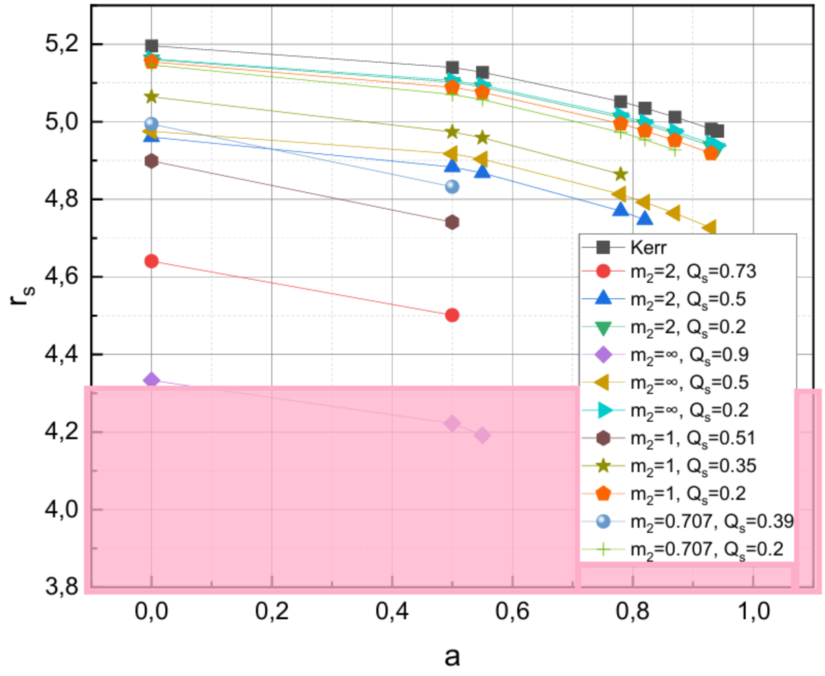

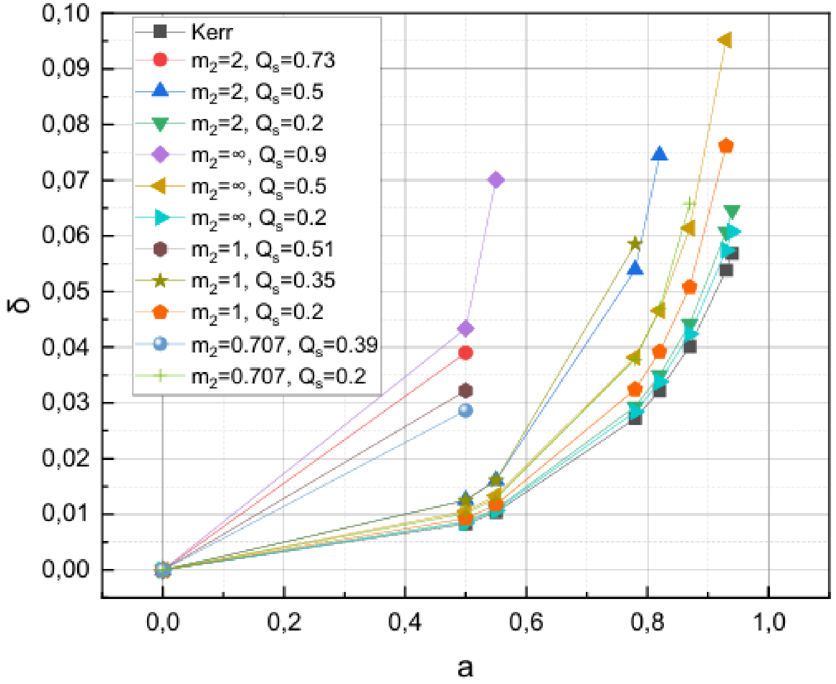

f

f (Q) Gravity

$$S[g,\Gamma] = \int d^4x \sqrt{-g}\mathbb{Q}.$$

$$A(r) = 1 - \frac{2M_{ren}}{r} - \alpha\frac{32}{r^2}$$

$$B(r)^{-1} = 1 - \frac{2M_{ren}}{r} - \alpha\frac{96}{r^2}$$

$$2M_{ren} = 2M - \alpha(\frac{32}{3M} + c_1),$$

-0,025<α<0,005

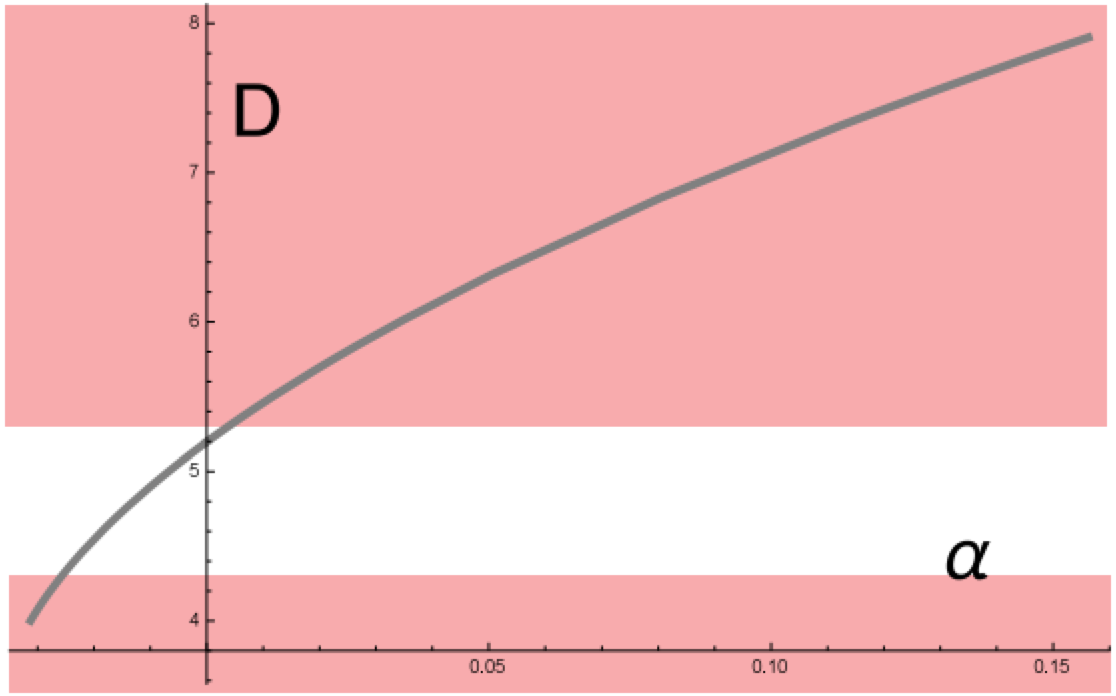

Рис. 2. The dependence of the shadow size D upon parameter α in $f(Q)$ gravity in M_{ren} units.

[8] Fabio D'Ambrosio, Shaun D. B. Fell, Lavinia Heisenberg, and Simon Kuhn. Black holes in $f(Q)$ Gravity. Physical Review D, 105(2), 2022.

Prokopov V. A., Alexeyev S. O., Zenin O. I. Black hole shadows constrain extended gravity 2: Sgr a* // *JETP*. — 2022.

f

f (Q) Gravity (rotation)

$$g_{tt} = -\frac{\rho^2 + A^2}{\rho^2},$$

$$g_{t\phi} = a \sin^2\theta \frac{A^2}{\rho^2},$$

$$g_{\theta\theta} = \rho^2,$$

$$g_{rr} = \frac{\rho^2}{r^2 + a^2 + A^2},$$

$$g_{\phi\phi} = \sin^2\theta \left(\rho^2 + a^2 \sin^2\theta \frac{\rho^2 - A^2}{\rho^2}\right),$$

$$A^2 = -2Mr + 96\alpha.$$

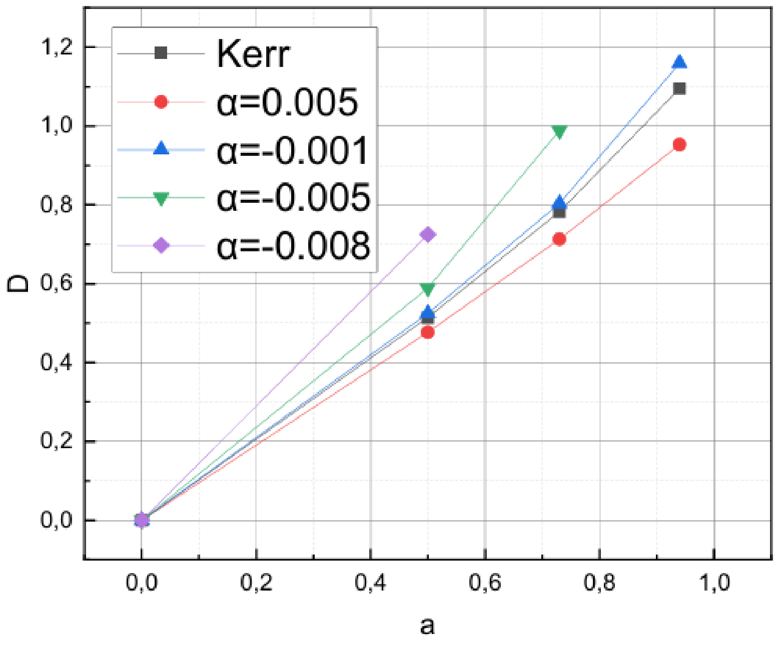

α=-0.001 a_{crit}=0.94

α=-0.005 a_{crit}=0.73

α=-0.008 a_{crit}=0.5

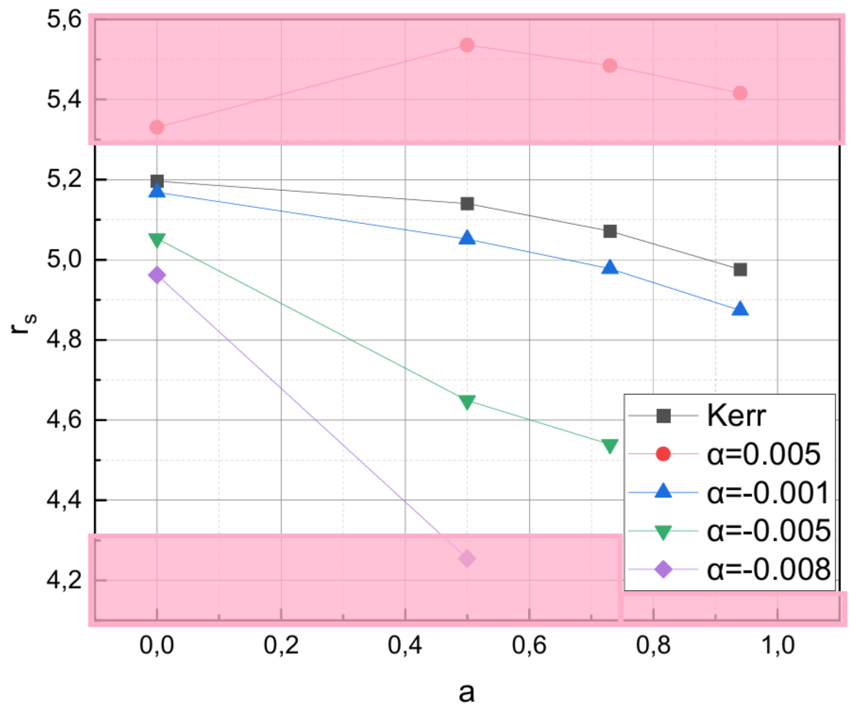

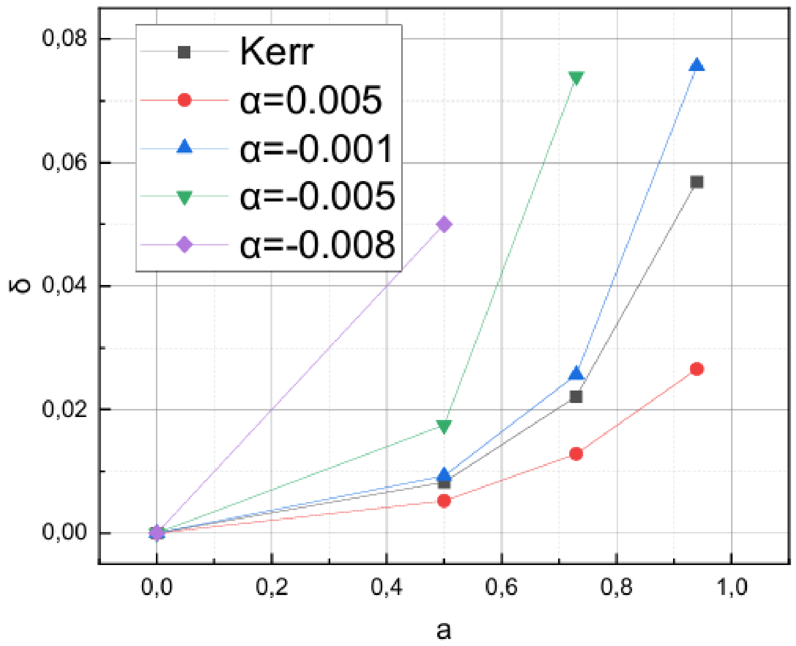

12

Discussion and conclusions

- Spherically symmetric solutions for extended gravity theories contain a number of additional parameters that are not present in the simplest solution of general relativity. Furthermore, these solutions, in addition to having one or more additional parameters, have a more complex structure compared to the Reissner-Nordström metric.

Discussion and conclusions

- Spherically symmetric solutions for extended gravity theories contain a number of additional parameters that are not present in the simplest solution of general relativity. Furthermore, these solutions, in addition to having one or more additional parameters, have a more complex structure compared to the Reissner-Nordström metric.
- The presence of additional parameters of the theory due to a more complex structure of the solution gives rise to the presence of critical values of the angular momentum a_{crit}. Such values exist in all theories considered, except for the Horndeski model and, partially, the Gauss-Bonnet scalar-tensor gravity (for $\xi<0.3$).

Discussion and conclusions

- Spherically symmetric solutions for extended gravity theories contain a number of additional parameters that are not present in the simplest solution of general relativity. Furthermore, these solutions, in addition to having one or more additional parameters, have a more complex structure compared to the Reissner-Nordström metric.
- The presence of additional parameters of the theory due to a more complex structure of the solution gives rise to the presence of critical values of the angular momentum $\boldsymbol{a}_{crit}$. Such values exist in all theories considered, except for the Horndeski model and, partially, the Gauss-Bonnet scalar-tensor gravity (for $\xi<0.3$).
- The previously made conclusion is confirmed that for some of the models considered, taking into account the parameters of the theory either slows down the rotation and the effects associated with it (this is most clearly manifested in the Horndeski theory and the Gauss-Bonnet scalar gravity), or enhances them (this is most clearly manifested in the Bumblebee model). For the other models considered, this effect is also present, but it works less linearly.

12

Discussion and conclusions

- Spherically symmetric solutions for extended gravity theories contain a number of additional parameters that are not present in the simplest solution of general relativity. Furthermore, these solutions, in addition to having one or more additional parameters, have a more complex structure compared to the Reissner-Nordström metric.
- The presence of additional parameters of the theory due to a more complex structure of the solution gives rise to the presence of critical values of the angular momentum a_{crit}. Such values exist in all theories considered, except for the Horndeski model and, partially, the Gauss-Bonnet scalar-tensor gravity (for $\xi<0.3$).
- The previously made conclusion is confirmed that for some of the models considered, taking into account the parameters of the theory either slows down the rotation and the effects associated with it (this is most clearly manifested in the Horndeski theory and the Gauss-Bonnet scalar gravity), or enhances them (this is most clearly manifested in the Bumblebee model). For the other models considered, this effect is also present, but it works less linearly.
- Considering the dependence of the shift parameter and its closeness to the Kerr value, we can conclude that the Horndeski, Bumblebee, and Gauss-Bonnet scalar gravity models work best and with a minimum number of additional parameters and restrictions as a basis for modeling black hole shadow profiles. Apparently, the best results should be expected from the Horndeski model. The Bumblebee model provides the best match with the Kerr metric.

Discussion and conclusions

- Spherically symmetric solutions for extended gravity theories contain a number of additional parameters that are not present in the simplest solution of general relativity. Furthermore, these solutions, in addition to having one or more additional parameters, have a more complex structure compared to the Reissner-Nordström metric.
- The presence of additional parameters of the theory due to a more complex structure of the solution gives rise to the presence of critical values of the angular momentum a_{crit}. Such values exist in all theories considered, except for the Horndeski model and, partially, the Gauss-Bonnet scalar-tensor gravity (for $\xi<0.3$).
- The previously made conclusion is confirmed that for some of the models considered, taking into account the parameters of the theory either slows down the rotation and the effects associated with it (this is most clearly manifested in the Horndeski theory and the Gauss-Bonnet scalar gravity), or enhances them (this is most clearly manifested in the Bumblebee model). For the other models considered, this effect is also present, but it works less linearly.
- Considering the dependence of the shift parameter and its closeness to the Kerr value, we can conclude that the Horndeski, Bumblebee, and Gauss-Bonnet scalar gravity models work best and with a minimum number of additional parameters and restrictions as a basis for modeling black hole shadow profiles. Apparently, the best results should be expected from the Horndeski model. The Bumblebee model provides the best match with the Kerr metric.
- Despite the less accurate modeling of shadow profiles than the first three metrics, we note that the Hayward metric (the metric of a black hole without a central singularity) is of additional interest, since in the framework of loop quantum gravity, it seems possible to get rid of both curvature singularities.